G3
Genes | Genomes | Genetics

A Genetic Screen Links the Disease-Associated Nab2 RNA-Binding Protein to the Planar Cell Polarity Pathway in *Drosophila melanogaster*

Wei-Hsuan Lee,* Edwin Corgiat,*,† J. Christopher Rounds,*,† Zenyth Shepherd,* Anita H. Corbett,‡ and Kenneth H. Moberg*,1

*Department of Cell Biology †Graduate Program in Genetics and Molecular Biology, and ‡ Department of Biology, Emory University, Atlanta, GA 30322

ORCID IDs: 0000-0002-0461-6895 (A.H.C.); 0000-0002-9820-5543 (K.H.M.)

ABSTRACT Mutations in the gene encoding the ubiquitously expressed RNA-binding protein ZC3H14 result in a non-syndromic form of autosomal recessive intellectual disability in humans. Studies in *Drosophila* have defined roles for the ZC3H14 ortholog, Nab2 (aka *Drosophila* Nab2 or dNab2), in axon guidance and memory due in part to interaction with a second RNA-binding protein, the fly Fragile X homolog Fmr1, and coregulation of shared Nab2-Fmr1 target mRNAs. Despite these advances, neurodevelopmental mechanisms that underlie defective axonogenesis in *Nab2* mutants remain undefined. *Nab2* null phenotypes in the brain mushroom bodies (MBs) resemble defects caused by alleles that disrupt the planar cell polarity (PCP) pathway, which regulates planar orientation of static and motile cells via a non-canonical arm of the Wnt/Wg pathway. A kinked bristle phenotype in surviving *Nab2* mutant adults additionally suggests a defect in F-actin polymerization and bundling, a PCP-regulated processes. To test for Nab2-PCP genetic interactions, a collection of PCP mutant alleles was screened for modification of a rough-eye phenotype produced by Nab2 overexpression in the eye (*GMR>Nab2*) and, subsequently, for modification of a viability defect among *Nab2* nulls. Multiple PCP alleles dominantly modify *GMR>Nab2* eye roughening and a subset rescue low survival and thoracic bristle kinking in *Nab2* zygotic nulls. Collectively, these genetic interactions identify the PCP pathway as a potential target of the Nab2 RNA-binding protein in developing eye and wing tissues and suggest that altered PCP signaling could contribute to neurological defects that result from loss of *Drosophila* Nab2 or its vertebrate ortholog ZC3H14.

Mutations in genes encoding RNA-binding proteins often lead to tissue-specific pathology, particularly within central nervous system (reviewed in Castello *et al.* 2013). Inactivating mutations in the human *ZC3H14* gene, which encodes a ubiquitously expressed poly(A) RNA-binding protein, are linked to a monogenic form of intellectual disability (reviewed in Fasken and Corbett 2016). Studies of murine ZC3H14 and its *Drosophila melanogaster* homolog, Nab2,

indicate that Nab2/ZC3H14 share a conserved function in brain neurons. Nab2 loss alters structure of the brain mushroom body (MB) lobes and impairs memory (Kelly *et al.* 2016; Bienkowski *et al.* 2017), while *ZC3H14* loss in mice alters hippocampal morphology and decreases working memory (Rha *et al.* 2017; Collins *et al.* 2019).

Drosophila Nab2 protein and its homologs in other species concentrate in the nucleus, with a small fraction of the protein also detected in the cytoplasm of various cell types, including neurons (Anderson *et al.* 1993; Leung *et al.* 2009; Van Den Bogaart *et al.* 2009; Guthrie *et al.* 2011; Bienkowski *et al.* 2017; Rha *et al.* 2017). Nuclear forms of Nab2/ZC3H14 proteins in various species are implicated in control of RNA poly(A) tail length, splicing, and export into the cytoplasm (Kelly *et al.* 2014; Soucek *et al.* 2016; Rha *et al.* 2017; Morris and Corbett 2018). In *Drosophila* neurons, cytoplasmic Nab2 localizes to messenger ribonucleoprotein particles (mRNPs) that contain the Fragile-X protein homolog Fmr1 and are implicated in

Allele	BDSC Stock #	Allele class (chr)	Allele transmission	Effect on GMR>Nab2	penetrance	# of F1 adults scored*	Notes on rationale
dsh^1	5298	hypomorph (X)	maternal	**E⁺** slight size	full	43m	carries w^a;K417M in DEP
			maternal	**S⁺⁺⁺** size,structure and pigment	full	48f	domain disrupts PCP (Axelrod,1998)
dsh^3	5299	amorph (X)	maternal	**S⁺⁺** structure,pigment slight size	full	34f	carries w^a;Δ534bp causing fs after N94 (Yanagawa,1995)
dsh^6	5297	amorph (X)	maternal	-	full	41f	carries w^a;lesion unknown (Perrimon,1987)
fz^1	1678	hypomorph (3)	maternal	**S⁺** size pigment	na	balancer issue**	Spontaneous, lesion unknown (Park,1994)
fz^{JB}	na	amorph(3)	paternal	**S⁺⁺** size,structure and pigment	partial	41m,46f	W355Ter in third TM domain (Povelones,2005)
$vang^{stbm153}$	6919	hypomorph (2)	paternal	-	full	23m,64f	Δ7bp causing fs after S205 (Wolff,1998)
$vang^{stbm6}$	6918	amorph (2)	paternal	**E⁺** slight size	na	42m,46f	Δ2bp causing fs after V81 (Wolff,1998)
$stan^{fz3}$	6967	hypomorph (2)	paternal	**S⁺** slight,structure and pigment	na	25m,67f	lesion unknown (Rawls,2003)
$stan^{e59}$	41776	amorph (2)	paternal	**E⁺** pigment loss **S⁺** size	full	46m,36f	Q1838Ter (Lu,1999)
pk^{30}	44229	Strong hypomorph (2)	paternal	**S⁺** slight,structure and pigment	full	52m,68f	Δ1306bp removes *pk* and *sple* function (Green,2000)
$pk^{pk-sple13}$	44230	hypomorph (2)	paternal	-	full	28m,40f	X-ray allele affecting *pk* and *sple* function (Gubb,1999)
$pk^{pk-sple14}$	na	hypomorph (2)	paternal	**S⁺** slight,size, and pigment	full	34m,41f	as above
$DAAM^A$	52348	lethal hypomorph (X)	maternal	**S⁺⁺⁺** size,structure and pigment	full	42f	D360V in FH3 domain (Haelterman,2014)
$DAAM^{G1567}$	33546	potential hypomorph (X)	maternal	**S⁺⁺** size pigment	full	52f	EP insertion into 5′ region (Belen,2004)
$Appl^d$	43632	amorph (X)	maternal	**S⁺⁺** structure pigment	full	34m	internal deletion
			maternal	**S⁺⁺⁺** structure pigment	full	29f	(Torroja,1996)
$Wnt4^{ems23}$	6650	amorph (2)	paternal	**S⁺⁺⁺** size,structure pigment	full	29m,37f	Q343 Ter (Cohen,2002)
$Wnt4^{c1}$	6651	hypomorph (2)	paternal	**S⁺** slight size	na	23m,34f	in-frame deletion of E299 (Cohen,2002)
$tap^{MI10541}$	55498	hypomorph	paternal	**S⁺⁺** size,structure pigment	full	54m,63f	MIC gene trap 5′ UTR (Nagarkar-Jaiswal,2015)
$puc^{MI11061}$	56272	hypomorph (3)	paternal	**S⁺⁺** size,structure pigment	full	58m,61f	MIC gene trap intron 3 (Nagarkar-Jaiswal,2015)
$Rbsn5^{X17}$	39628	amorph (2)	paternal	**S⁺** slight size	na	20m,27f	Q241 Ter (Morrison,2008)
$Pabp2^{55}$	39628	amorph (2)	paternal	**E⁺⁺⁺** semi-lethal	full	8m,5f	Deletion of coding sequence (Benoit,2005)

mRNA translational repression (Bienkowski *et al.* 2017). Murine ZC3H14 also localizes to the neuronal cytoplasm, where it co-sediments with puromycin-sensitive ribosomal fractions and localizes to axons and dendritic spines (Rha *et al.* 2017). These data indicate that Nab2/ZC3H14 likely has effects on nuclear pre-mRNA processing and cytoplasmic translation of mRNAs involved in neurodevelopment.

The majority of Nab2-regulated neuronal mRNAs are undefined, but animals lacking *Nab2* share defects in the brain mushroom bodies (MBs) with mutants in one of four genes encoding components of planar cell polarity (PCP) pathway (*disheveled*, *prickle*, *frizzled* and *Van Gogh*) (Ng 2012; Kelly *et al.* 2016), suggesting a potential Nab2-

PCP link in the brain. The PCP pathway involves two apically localized transmembrane complexes, Starry Night (also Flamingo)-Van Gogh-Prickle (Stan-Vang-Pk) and Starry night-Frizzled-Dishevelled-Diego (Stan-Fz-Dsh-Dgo), that interact across cell:cell junctions but are mutually antagonistic within cells, resulting in a polarized pattern of complex accumulation that propagates across an epithelium (reviewed in Yang and Mlodzik 2015). PCP controls the planar orientation of cells via localized effects on the F-actin cytoskeleton and contributes to a number of developmentally programmed processes, including proximal-distal hair cell orientation and axon guidance in the nervous systems of multiple species (Sato *et al.* 2006; Srahna *et al.* 2006;
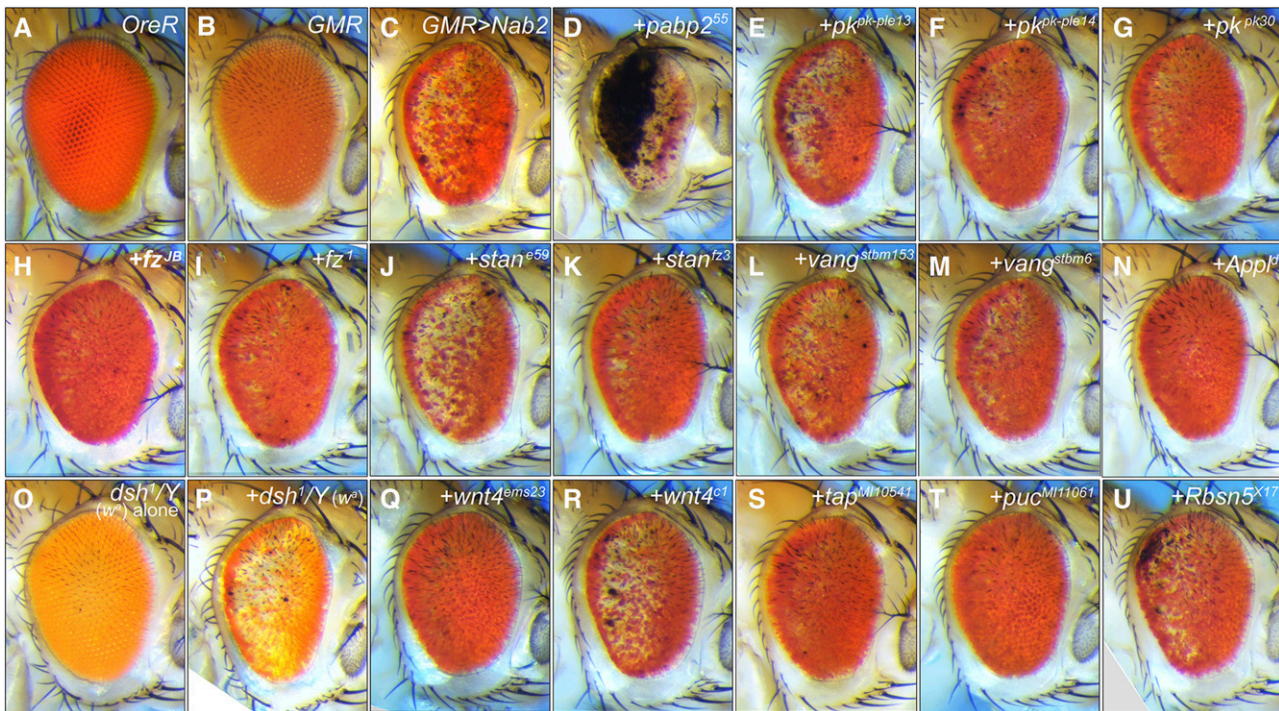
G3 Genes | Genomes | Genetics

Figure 1 *GMR>Nab2* male eye modification by Wg/PCP alleles. Images of adult male eyes oriented posterior (left) to anterior (right): (A) *wildtype* control (*OreR*), (B) *GMR-Gal4* alone, (C) *GMR>Nab2* alone, or combined with (D) *pabp2⁵⁵/+* (positive control as in Pak *et al.* 2011), and (E-U) the indicated Wg/PCP alleles. The (O) *wᵃ,dsh¹/Y* eye (BDSC #5298) is provided as a control for the apricot eye color and PCP-defective genetic background of the (P) *wᵃ,dsh¹/Y, GMR>Nab2* genotype. Images to scale.

Inaki *et al.* 2007; Hollis and Zou 2012; Ng 2012; Vandewalle *et al.* 2013; Ackley 2014; Gombos *et al.* 2015; Avilés and Stoeckli 2016).

To investigate a Nab2-PCP link *in vivo*, a group of alleles of core and accessory PCP components was screened for modification of phenotypes produced by eye-specific *Nab2* overexpression (*GMR>Nab2*) (Pak *et al.* 2011). This candidate approach identifies multiple PCP alleles that dominantly interact with *GMR>Nab2*, and a subset of PCP alleles that also modify *Nab2* loss-of-function phenotypes. A PCP-Nab2 link is further supported by our discovery that *Nab2* mutant adults exhibit wing hair misorientation, a feature of many *Drosophila* PCP factors (reviewed in Yang and Mlodzik 2015). Collectively, these data identify the PCP pathway as a potential target of the Nab2 RNA binding protein in neurons.

MATERIALS AND METHODS

Drosophila genetics:

Crosses were maintained in 25° humidified Shel•Lab incubators with 12hr light-dark cycles. The *Nab2* alleles *ex3* (null), *pex41* (control, *precise excision 41*), and the *EP3716* line carrying *UAS* sites upstream of the *Nab2* coding sequence, have been described previously (Pak *et al.* 2011). For autosomal alleles, five males of each candidate modifier stock ('paternal transmission' in Table 1; balancers correspond to those listed for each BDSC stock) were crossed to five virgin *GMR>Nab2* females (*w-;GMR-Gal4/CyO;Nab2^EP3716/TM6B,tub-Gal80*). For X-linked lethal alleles and the two X-linked viable alleles, five virgin females of each candidate modifier stock ('maternal transmission' in Table 1; balancers correspond to those listed for each BDSC stock, except for *dsh⁶*, *dsh¹* and *Appl^d* chromosomes, which were rebalanced over *FM7a*) were crossed to five *GMR>Nab2* males (*w-/Y;GMR-Gal4/CyO;Nab2^EP3716/TM6B,tub-Gal80*). Three

independent crosses were set up per genotype. Lines obtained from Bloomington *Drosophila* Stock Center (BDSC): *GMR-Gal4*, *dsh¹* (Axelrod *et al.* 1998), *dsh³* (Yanagawa *et al.* 1995), *dsh⁶* (Perrimon and Mahowald 1987), *fz¹* (Park *et al.* 1994), *fz^JB* (Povelones *et al.* 2005), *vang^stmb153* and *vang^stbm6* (Wolff and Rubin 1998), *stan^fz3* (Rawls and Wolff 2003) *stan^e59* (Lu *et al.* 1999), *pk³⁰* (Green *et al.* 2000), *pk^pk-sple13* (Gubb *et al.* 1999), *DAAM^A* (Haelterman *et al.* 2014), *DAAM^G1567* (Bellen *et al.* 2004), *Appl^d* (Torroja *et al.* 1999), *wnt4^ems23* and *wnt4^c1* (Cohen *et al.* 2002), *tap^MI10541* and *puc^MI11061* (Nagarkar-Jaiswal *et al.* 2015), *Rbsn5^x17* (Morrison *et al.* 2008), *Pabp2⁵⁵* (Benoit *et al.* 2005). *fz^JB* and *pk^pk-sple14* alleles were a gift of G. Pierre-Louis (present address Valencia College, FL) and J. Axelrod.

Image and data collection

Images of adult eyes were captured with a Leica MC-170 HD digital camera mounted on a Nikon SMZ800N microscope and processed with Adobe Photoshop to standardize brightness and sharpness. Eye phenotypes were categorized as 'Enhancer (E)', 'Suppressor (S)', or 'no effect (-)' based on visual assessment of pigmentation loss, disorganization of the retinal honeycomb structure, and quantitative measure of 2D eye size (see Table 1 and Figure 3). Eye size was determined for five eyes per condition (*i.e.*, genotype and gender) using Photoshop and standardized to the average size of five *GMR-Gal4* control eyes (males in Figure 3A and females in Figure 3B). For survival assays in Figure 4A-B, 100 non-Tubby female larvae were collected in triplicate from an intercross of *Nab2^ex3/TM6B^Tb,Hu* or *Nab2^pex41* ('control') animals, transferred to a fresh vial, and allowed to pupate. Viability was assessed by manual counting of viable, eclosed adults. Survival was calculated as the number of observed adults over the total number of larvae. For modifier alleles, *Nab2^ex3/TM6B^Tb,Hu* females balanced for the indicated Wg/PCP allele (*e.g.*, *dsh¹/FM7i,Actin-GFP*,
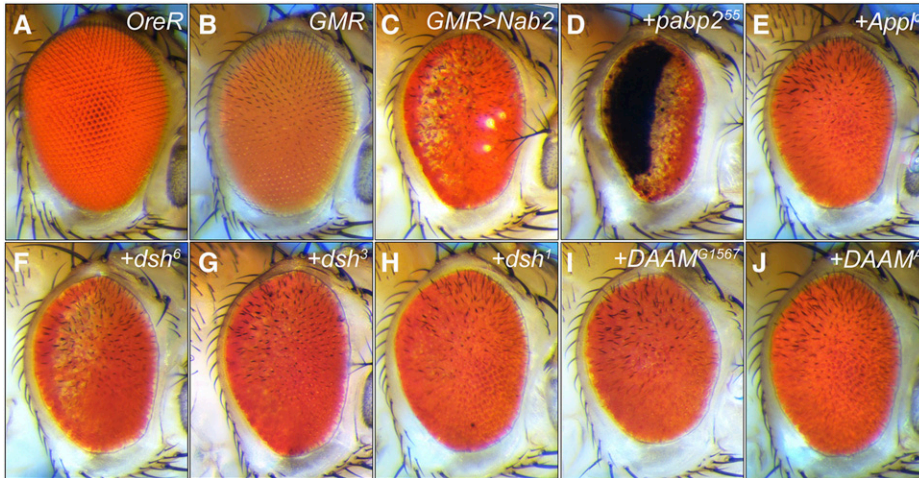
Figure 2 *GMR>Nab2* female eye modification by Wg/PCP alleles. Images of adult female eyes oriented posterior (left) to anterior (right): (A) *wildtype* control (*OreR*), (B) *GMR-Gal4* alone, (C) GMR>Nab2 alone, or combined with (D) *pabp2^55^/+* (positive control as in Pak *et al.* 2011), and (E-J) the indicated X-linked Wg/PCP alleles. Images to scale.

Appl^d^/FM7,Actin-GFP, *pk^pk-sple14^/CyO,Dfd-GFP*, or *Wnt4^c1^/CyO,Dfd-GFP*) were crossed to *Nab2^ex3^/TM6B^Tb,Hu^* males, and the viability of *modifier/+;Nab2^ex3^/Nab2^ex3^* females was determined by manual counting of viable adults as described above. To calculate the penetrance of bristle kinking in Figure 5, control (*Nab2^pex41^*), *Nab2^ex3^*, and *dsh^1^/+;;Nab2^ex3^* females collected from crosses described above were examined for kinking of humeral and scutal macrochaetae characteristic of *Nab2^ex3^* adults (Pak *et al.* 2011). Females with at least one kinked thoracic bristle were scored as 'positive' for the phenotype. Kinking penetrance was determined by dividing the percent of adult females with kinked bristles over the total number of adult females observed.

Statistical analysis

One-way ANOVA was used to compute significance values (*p*-values indicated in Legends and denoted by asterisks*) for eye size data, survival data, and bristle kink data. PrismGraphPad Software was used to generate graphs and perform statistical tests. Sample sizes (n) and p-values are indicated in figures or legends. Modifying effects of PCP alleles on *Nab2^ex3^* adult viability were quantified by as observed adult *vs.* expected adults (set as 100%) among three replicates of 100 sorted female larvae.

Data availability

All *Drosophila* transgenic and mutant lines used in this study are freely available upon request.

RESULTS

PCP alleles dominantly modify the GMR>Nab2 eye phenotype

As described in prior work (Pak *et al.* 2011), overexpression of *Nab2* in developing eye tissue with a *GMR-Gal4* transgene (chromosome 2) and an EP-type transposon located in the first non-coding exon of *Nab2* (*GMR-Gal4, Nab2^EP3716^*; hereafter '*GMR>Nab2*'), leads to adult eyes that are rough, reduced in size, and lack red pigmentation in posterior domains relative to wildtype *Oregon-R* (*OreR*) or '*GMR* only' control eyes. These phenotypes are more severe in males (Figures 1A-C) than females (Figures 2A-C) and provide a useful background to screen for alleles that dominantly interact with *Nab2*. This approach has proven effective in identifying factors that interact functionally or physically with Nab2, including the nuclear poly(A)

binding protein Pabp2 (included as a positive control in Figures 1D and 2D) (Pak *et al.* 2011) and the disease-associated RNA-binding protein Fmr1 (see Bienkowski *et al.* 2017).

To use the *GMR>Nab2* transgenic system to assess genetic interactions between Nab2 and PCP factors, a group of twenty (20) alleles corresponding to core and accessory PCP factors (Table 1) was crossed into the *GMR>Nab2* background and scored for modification of eye size, roughening, and pigmentation in the F1 progeny. Fourteen autosomal alleles were screened in *GMR>Nab2* males (Figure 1E-U), and four X-linked lethal alleles of the Wg/PCP factors *disheveled* (*dsh^3^*, *dsh^6^*) and *Dishevelled Associated Activator of Morphogenesis* (*DAAM^G1567^*, *DAAM^A^*) were tested as heterozygotes in *GMR>Nab2* females (Figure 2E-J). Two viable X-linked mutant alleles, *dsh^1^* and *Amyloid precursor protein-like^d^* (*Appl^d^*), were tested both as hemizygotes in males (Figure 1N,P) and heterozygotes in females (Figure 2E,H). As summarized in Table 1, seventeen of the alleles modified, to varying degrees, one of the three *GMR>Nab2* eye phenotypes tracked in this study: loss of pigmentation, disorganized ommatidial structure, and reduced eye size. Modification of the first two phenotypes was assessed by visual inspection, while the effect on male and female eye size was determined by measuring two-dimensional (2D) eye size in fixed images (Figures 3A, B). Nine of the alleles produced moderate (S++) or strong suppression (S+++) of one or more of the three scored *GMR>Nab2* phenotypes: *dsh^3^*, *frizzled^JB^* (*fz^JB^*), *DAAM^A^*, *DAAM^G1567^*, *Appl^d^*, *Wnt oncogene analog-4^ems23^* (*Wnt4^ems23^*), *target of Poxn^MI10541^* (*tap^MI10541^*), and *puckered^MI11061^* (*puc^MI11601^*). One allele, *vang^stbm6^*, mildly enhanced (E+) *GMR>Nab2* and six alleles mildly suppressed (S+) one or more of the *GMR>Nab2* phenotypes: *fz^1^*, *starry night^fz3^* (*stan^fz3^*), *pk^30^*, *pk^pk-sple14^*, *Wnt4^c1^*, and *Rbsn5^X17^*. One allele, *stan^e59^*, mildly enhanced *GMR>Nab2* pigment loss, but also mildly suppressed the reduced eye size. Finally, the *dsh^1^* allele suppressed eye size, pigment loss and roughness in *dsh^1^/+* heterozygous females, but had a mild enhancing effect on *GMR>Nab2* in hemizygous males (*i.e.*, *dsh^1^/Y*), although this phenotype was more difficult to score based on the apricot eye color of the *w^a^* allele (Morgan *et al.* 1925) carried on the *dsh^1^* chromosome (see Figure 1C *vs.* O,P). Overall, of the twenty tested Wg/PCP alleles, only three, *dsh^6^*, *vang^stmb153^* and *pk^pk-sple13^*, had no effect on *GMR>Nab2* eye phenotypes.

A review of the alleles with modifying effects is consistent with a link between Nab2 and the Wg/PCP pathway. Two of three *dsh* alleles tested (*dsh^1^* and *dsh^3^*) suppressed the female *GMR>Nab2* phenotype
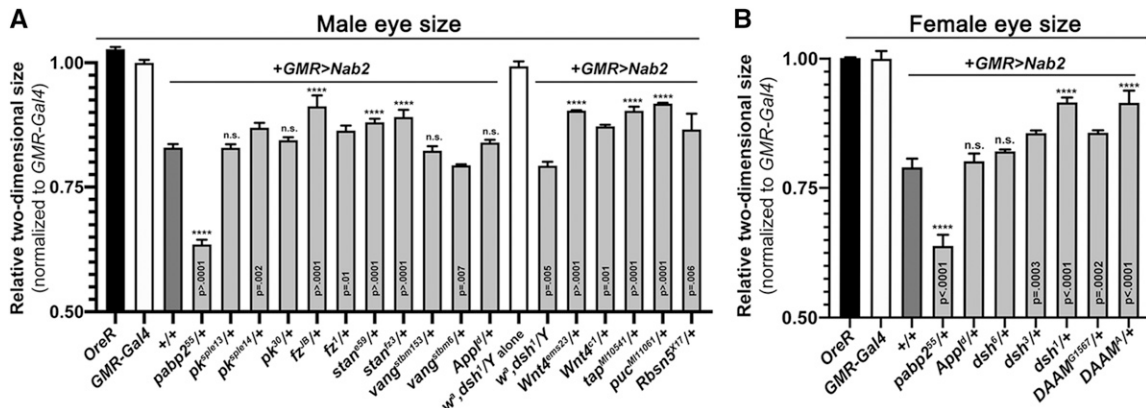
Figure 3 Effect of Wg/PCP alleles on two-dimensional size of *GMR>Nab2* eyes. Quantitation of 2D eye size in adult (A) males or (B) females carrying the indicated alleles. Pixel number was determined for five eyes per test genotype using Photoshop and normalized to five *GMR-Gal4* control eyes. Asterisks denote modification with P<0.0001. Other p values are noted. 'n.s.' = not significant. Errors bars represent SEM.

as heterozygotes. The *dsh³* amorph carries an internal deletion that causes a frameshift after codon 94 (Yanagawa *et al.* 1995), and the *dsh¹* hypomorph selectively blocks PCP signaling due to an amino acid substitution in the DEP domain (Disheveled, Egl-10, P leck-strin) (Axelrod *et al.* 1998; Boutros *et al.* 1998; Penton *et al.* 2002). *GMR>Nab2* male eyes are mildly enhanced by *dsh¹/Y* hemizygosity, perhaps due to a requirement for residual wildtype Dsh function to modify Nab2 phenotypes or to a sex-specific interaction between *dsh¹* and *GMR>Nab2*. Both *fz* alleles tested act as dominant suppressors, and the *fzᴶᴮ* amorph is a stronger suppressor than the *fz¹* hypomorph. *stanᶠᶻ³* is also a suppressor, although a second allele, *stanᵉ⁵⁹*, has mild enhancing and suppressing effects on *GMR>Nab2* phenotype. Among *pk* alleles tested, *pk³⁰* (also *Df(2R)pk*) and *pkᵖᵏ⁻ˢᵖˡᵉ¹⁴* mildly suppress, while a third allele, *pkᵖᵏ⁻ˢᵖˡᵉ¹³*, has no obvious effect on *GMR>Nab2* eyes.

Alleles of PCP accessory factors also strongly modify the *GMR>Nab2* phenotype. Two alleles of the X-linked Dsh-interactor *DAAM* act as strong dominant suppressors of *GMR>Nab2* eye phenotypes; one of these suppressors, *DAAMᴬ*, contains a D360V substitution in the formin-homology 3 (FH3) domain (Haelterman *et al.* 2014) that is predicted to disrupt interactions with Rac GTPases during axonal outgrowth (Gombos *et al.* 2015). The suppressor allele *Applᵈ* (β-Amyloid protein precursor-like) is an amorph that deletes the central coding region of a transmembrane protein that acts as a PCP-accessory factor in neurons and has established roles in retinal axon pathfinding and synapse formation (Luo *et al.* 1992; Ashley *et al.* 2005; Mora *et al.* 2013; Soldano *et al.* 2013). The amorphic allele *Wnt4ᵉᵐˢ²³*, which encodes a Fz ligand with roles in canonical and non-canonical Wg/Wnt signaling (Cohen *et al.* 2002), is a strong suppressor, while the weak hypomorph *Wnt4ᶜ¹* has a much weaker effect. Viable *P*-element insertions in the *puc* (*pucᴹᴵ¹¹⁰⁶⁰*) and *tap* (*tapᴹᴵ¹⁰⁵⁴¹*) loci, which respectively encode a component of the PCP-regulated JNK pathway (Boutros *et al.* 1998; Martin-Blanco *et al.* 1998) and a regulator of Dsh levels in brain mushroom body (MB) neurons (Yuan *et al.* 2016), also act as *GMR>Nab2* suppressors. Finally, a mutant allele of the endocytic factor *Rabenosyn-5* (*Rbsn5*), which regulates polarized distribution of PCP proteins in wing cells (Mottola *et al.* 2010) has a mild suppressive effect on the size of *GMR>Nab2* eyes. In sum, these data reveal a series of genetic interactions which are consistent with a model in which reducing PCP activity partially mitigates the effect of Nab2 overexpression in the developing eye.
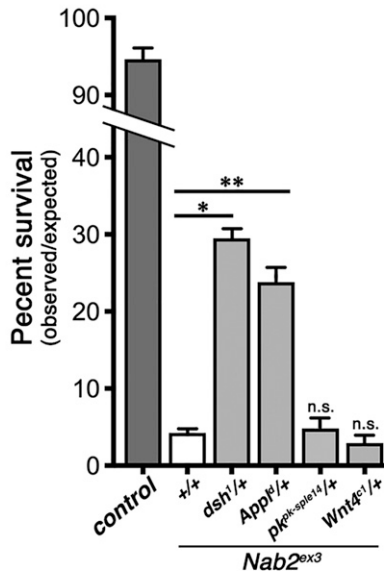
PCP alleles dominantly modify Nab2 loss of function phenotypes

The genetic interactions between multiple PCP alleles and the *GMR>Nab2* overexpression transgene prompted analysis of PCP allele interactions with the *Nab2* loss-of-function (LOF) allele *Nab2ᵉˣ³*, a recessive amorph that causes defects in survival, lifespan, locomotion, thoracic bristle morphology, and neurodevelopment (Pak *et al.* 2011; Kelly *et al.* 2016). Four different PCP alleles – three suppressor alleles, *dsh¹*, *Applᵈ*, *pkᵖᵏ⁻ˢᵖˡᵉ¹⁴*, and one weak modifier allele, *Wnt4ᶜ¹* - were tested for dominant effects on two readily scored *Nab2ᵉˣ³* null phenotypes: reduced survival to eclosion (<5% in past studies *e.g.*, Pak *et al.* 2011), and thoracic bristle kinking. The *Nab2ᵉˣ³* survival defect was chosen because it is rescued by neuron-specific expression of either fly *Nab2* or human *ZC3H14* (Kelly *et al.* 2016), suggesting that it is an indicator of a conserved requirement for Nab2 in neurons. The *Nab2ᵉˣ³* thoracic bristle defect was chosen because it suggests a link to the PCP-regulated processes of F-actin assembly and bundling (reviewed in Adler and Wallingford 2017).

To analyze adult viability, the percent of pupae eclosing into viable adults was calculated among 100 non-Tubby female larvae collected from an intercross of *Nab2ᵉˣ³/TM6Bᵀᵇ,ᴴᵘ* adults. Consistent with our prior work (*e.g.*, Pak *et al.* 2011), approximately 3–5% of *Nab2ᵉˣ³* zygotic null females eclose as viable adults, while *Nab2ᵖᵉˣ⁴¹* control females (aka *Nab2ʷᵗ*; a precise excision of the *EP3716 P*-element that was used to generate *Nab2ᵉˣ³*) display essentially full viability (~94% eclosion) (Figure 4A-B). The X-linked *dsh¹* and *Applᵈ* alleles respectively rescue *Nab2ᵉˣ³* female survival to ~30% and ~25% when inherited through *FM7a*-balanced heterozygous mothers. Heterozygosity for either the *pkᵖᵏ⁻ˢᵖˡᵉ¹⁴* or *Wnt4ᶜ¹* alleles has no significant effect on *Nab2ᵉˣ³* female survival. These genetic data demonstrate that two PCP alleles that modify *GMR>Nab2*, *dsh¹* and *Applᵈ*, also dominantly rescue the partial lethality of *Nab2ᵉˣ³* females. This viability rescue in *dsh¹/+;;Nab2ᵉˣ³* surviving adult females is also associated with rescue of thoracic bristle kinking compared to *Nab2ᵉˣ³* null females (~45% *vs.* ~90%; calculated as fraction of individuals showing at least one kinked humeral or scutal bristle) (Figure 5A-B).

The ability of PCP alleles to modify phenotypes associated with Nab2 gain (*GMR>Nab2*) and loss (*Nab2ᵉˣ³*) prompted an assessment of whether *Nab2* loss is sufficient to produce PCP-like defects in sensitive tissues *e.g.*, altering proximal-distal wing hair orientation (Yang and Mlodzik 2015). To test this hypothesis, hairs in a fixed

Figure 4 Effect of four Wg/PCP alleles on survival of *Nab2* null females. (A) Quantification of female eclosion rates among *wildtype* controls (dark gray fill; *Nab2^pex41*), *Nab2^ex3* homozygotes (white fill), or *Nab2^ex3* homozygotes that are also heterozygous for *dsh^1*, *Appl^d*, *pk^pk-sple-14* or *Wnt4^c1* (gray fill). Data are presented as the percentage of viable females (observed) *vs.* the total number of pupae tracked (expected) from three biological replicates of 100 sorted female larvae shown in (B) (also see Materials and Methods). Statistical significance is indicated (*p=0.0002; **p=0.0005; n.s. = not significant). Error bars represent SEM.

region between L3-L4 veins and distal to the posterior cross vein (PCV) were imaged in control (*Nab2^pex41*) and *Nab2^ex3* adult female wings (Figures 5C-D). Three examples of adult wing hair morphology in the L3-L4 region are provided for each genotype, together with corresponding magnified insets. Wing hairs in control wings are arrayed in a uniform right-to-left orientation that matches the proximal-to-distal axis of the wing (Figure 5C); by contrast, hairs in *Nab2^ex3* wings exhibit orientation defects (Figure 5D), including misrotated hairs and occasional evidence of coordinated misrotation among adjacent hair cells (*e.g.*, Figure 5D, inset in top panel). These PCP-like effects in *Nab2* null females provide evidence of a role for Nab2 in orientating adult wing hairs that is consistent with dominant genetic interactions detected between PCP mutant alleles and a *Nab2* LOF allele and a *UAS-Nab2* transgene.

DISCUSSION

Here we have used three phenotypes caused by altered dosage of the *Drosophila* poly(A) RNA-binding protein Nab2, (1) eye roughness caused by overexpression of *Nab2* (*GMR>Nab2*), (2) a neuronal requirement for *Nab2* in adult survival and (3) thoracic bristle kinking in *Nab2* null animals, to screen for genetic interactions between *Nab2* and genes encoding components of the Wg/planar

cell polarity (PCP) pathway. The *Nab2*-PCP interactions detected by this approach are consistent with a role for Nab2 in restraining PCP signaling in *Drosophila* tissues, perhaps by inhibiting expression of a PCP component. Given that PCP signaling and Nab2/ZC3H14 are each linked to axon guidance (Sato *et al.* 2006; Srahna *et al.* 2006; Inaki *et al.* 2007; Pak *et al.* 2011; Hollis and Zou 2012; Ng 2012; Vandewalle *et al.* 2013; Ackley 2014; Kelly *et al.* 2014; Gombos *et al.* 2015; Avilés and Stoeckli 2016; Kelly *et al.* 2016; Bienkowski *et al.* 2017; Rha *et al.* 2017; Collins *et al.* 2019), these data argue that neurodevelopmental defects in flies, mice, and humans lacking Nab2/ZC3H14 may arise in part due to altered PCP signaling.

Alleles that impair Wg/PCP signaling, and in some cases specifically perturb PCP (*e.g.*, *dsh^1*, *Appl^d*, *DAAM^A*), are able to suppress phenotypes caused by either *Nab2* overexpression (*GMR>Nab2*) or loss (*Nab2^ex3*). This pattern differs from other *Nab2* modifier alleles that have inverse effects in *Nab2* gain *vs.* loss backgrounds *e.g.*, *dfmr1^Δ50* (as in Bienkowski *et al.* 2017), and could be explained if Nab2 modulates levels of a PCP factor(s). Since overexpression and loss-of-function of some PCP factors, like Frizzled, produce similar disruptions to polarity (reviewed in Yang and Mlodzik 2015), gain and loss of Nab2 might also be expected to have similar effects on PCP that are suppressed by Wg/PCP alleles. Imbalanced PCP signaling resulting from Nab2 overexpression or loss would then be restored by reducing the genetic dose of Wg/PCP factors. The suppressive effects of Wg/PCP amorphs like *dsh^3* and *fz^JB* do not distinguish whether Nab2 could affect one or both arms of the Wg/PCP pathway. The suppressive effect of the *dsh^1* allele, which specifically impairs PCP signaling (Axelrod *et al.* 1998), provides evidence of a Nab2 link to the PCP pathway. If this link is strong enough, then *Nab2* null flies might thus be expected to display defects in hallmark PCP-regulated processes, *e.g.*, wing hair polarization and ommatidial rotation. Consistent with this hypothesis, we document moderate hair misorientation defects in *Nab2* null adult wings, suggesting that Nab2 may regulate PCP activity in this tissue. Nab2 is expressed ubiquitously but required in neurons for viability (Kelly *et al.* 2014); thus, the rescue of *Nab2* null viability by *dsh^1* also implies that a Nab2-PCP link may also occur in neurons. This idea is further supported by the genetic interaction between *Nab2^ex3* and the *Appl^d* allele, which inactivates a neuron-specific PCP component (Soldano *et al.* 2013) and by *GMR>Nab2* modification by an allele of *tap*, a regulator of Dsh expression in neurons (Yuan *et al.* 2016). Interestingly, *Nab2* and PCP alleles individually alter the trajectories of mushroom body axons that project from Kenyon cells (Ng 2012; Kelly *et al.* 2016), which provides a cellular context for future study of a Nab2-PCP interaction.

Nab2 may modify PCP-regulated developmental processes indirectly through post- transcriptional control of proteins (or a protein) that is not core PCP components but regulates a common process (*e.g.*, via F-actin bundling). Alternatively, Nab2 may directly regulate post-transcriptional expression of a core PCP component. In this regard, it is notable that levels of the Vang family member Vangl2 are elevated in the hippocampal proteome of *Zc3h14* knockout mice (Rha *et al.* 2017), and that depletion of ZC3H14 from cultured N2A cells leads to intron retention in the *PSD95* mRNA (Morris and Corbett 2018), which encodes a postsynaptic guanylate kinase required for activity-dependent synaptic plasticity (reviewed in Xu 2011). Intriguingly, the fly PSD95 homolog Discs Large-1 (Dlg1) controls canonical Wg signaling in wing tissue by stabilizing Dsh protein (Liu *et al.* 2016). In light of these observations in mammalian systems, the corresponding *Drosophila* mRNAs *vang* and *dlg1*
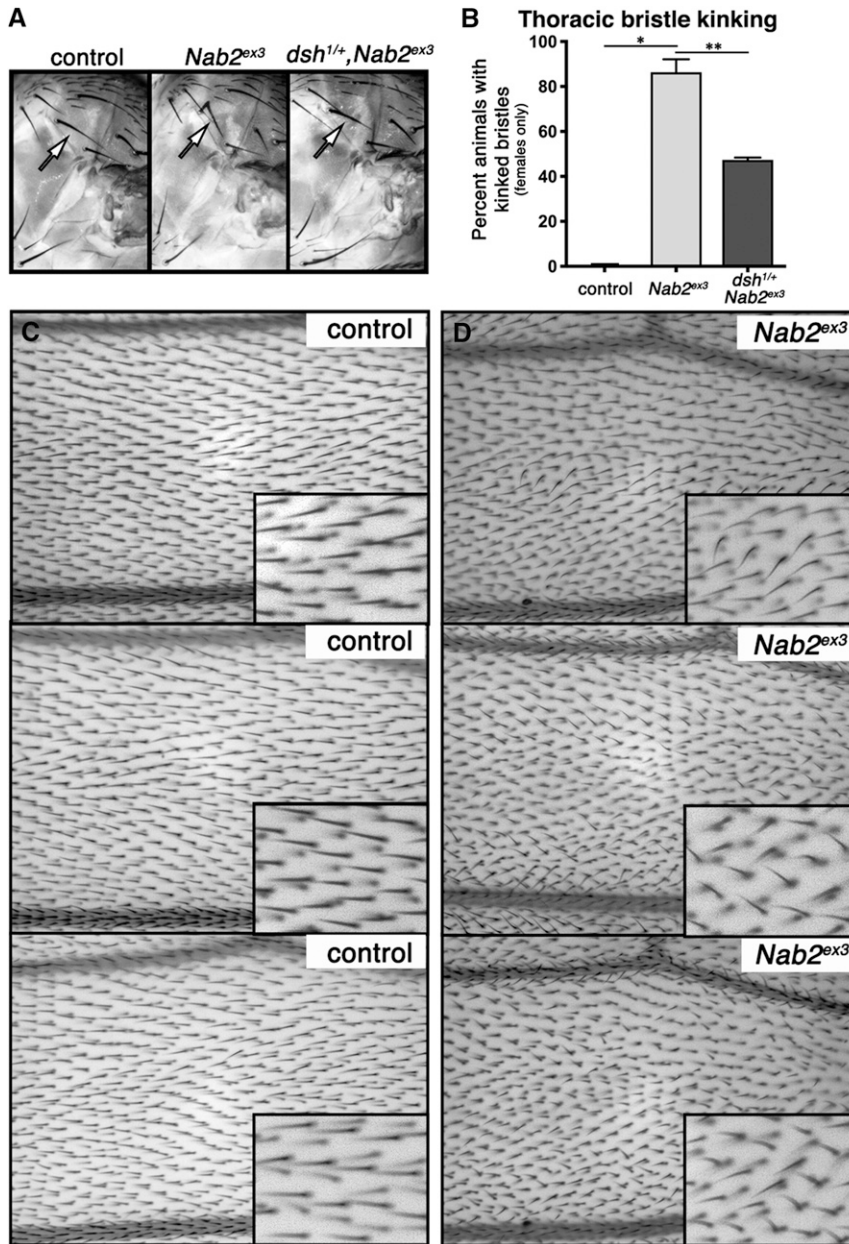
Figure 5 *Nab2ex3* effects on bristle morphology and wing hair orientation. (A) Examples of humeral bristle morphology (arrows) in a *wildtype* control (*Nab2pex41*), *Nab2ex3* homozygote and *dsh1/+;;Nab2ex3* adult female. (B) Frequency of bristle kinking in *wildtype* controls (*Nab2pex41*), *Nab2ex3* homozygotes (gray fill) or *dsh1/+;;Nab2ex3* (dark gray fill) adult females. Data are presented as the percentage of viable females with at least one kinked humeral or scutal bristle *vs.* the total number of eclosed females counted from three biological replicates of 100 sorted female larvae (see Materials and Methods). Statistical significance is indicated (*p=0.0003; **p=0.02). (C-D) Images of wing hairs in the L3-L4 region from three representative examples of control (*Nab2-pex41*) or *Nab2ex3* adult female wings orientated proximal to distal (right to left). Insets (lower right) show magnified views from each panel.

represent candidate Nab2 targets that may contribute to Nab2-PCP genetic interactions documented in this study.

In summary, we have carried out a candidate-based genetic screen that has identified a series of dominant genetic interactions between Wg/PCP alleles and both a *Nab2* overexpression transgene and null allele. Based on data cited above, these genetic data support a molecular model in which Nab2 may regulate expression of a PCP protein or proteins in different cell types, including neurons and wing hair cells. This hypothesis is significant given that very few Nab2-target mRNAs are known and the Nab2 human ortholog ZC3H14 is lost in an inherited form of recessive intellectual disability (Pak *et al.* 2011). Thus, the work presented here is a key first step in exploring conserved functional and molecular links between Nab2/ZC3H14 and PCP activity that may contribute to a conserved requirement for Nab2/ZC3H14 in neurodevelopment.

LITERATURE CITED

Ackley, B. D., 2014   Wnt-signaling and planar cell polarity genes regulate axon guidance along the anteroposterior axis in C. elegans. Dev. Neurobiol. 74: 781–796. https://doi.org/10.1002/dneu.22146

Adler, P. N., and J. B. Wallingford, 2017   From Planar Cell Polarity to Ciliogenesis and Back: The Curious Tale of the PPE and CPLANE

proteins. Trends Cell Biol. 27: 379–390. https://doi.org/10.1016/j.tcb.2016.12.001

Anderson, J. T., S. M. Wilson, K. V. Datar, and M. S. Swanson, 1993 NAB2: a yeast nuclear polyadenylated RNA-binding protein essential for cell viability. Mol. Cell. Biol. 13: 2730–2741. https://doi.org/10.1128/MCB.13.5.2730

Ashley, J., M. Packard, B. Ataman, and V. Budnik, 2005 Fasciclin II signals new synapse formation through amyloid precursor protein and the scaffolding protein dX11/Mint. J. Neurosci. 25: 5943–5955. https://doi.org/10.1523/JNEUROSCI.1144-05.2005

Avilés, E. C., and E. T. Stoeckli, 2016 Canonical wnt signaling is required for commissural axon guidance. Dev. Neurobiol. 76: 190–208. https://doi.org/10.1002/dneu.22307

Axelrod, J. D., J. R. Miller, J. M. Shulman, R. T. Moon, and N. Perrimon, 1998 Differential recruitment of Dishevelled provides signaling specificity in the planar cell polarity and Wingless signaling pathways. Genes Dev. 12: 2610–2622. https://doi.org/10.1101/gad.12.16.2610

Bellen, H. J., R. W. Levis, G. Liao, Y. He, J. W. Carlson et al., 2004 The BDGP gene disruption project: single transposon insertions associated with 40% of Drosophila genes. Genetics 167: 761–781. https://doi.org/10.1534/genetics.104.026427

Benoit, B., G. Mitou, A. Chartier, C. Temme, S. Zaessinger et al., 2005 An essential cytoplasmic function for the nuclear poly(A) binding protein, PABP2, in poly(A) tail length control and early development in Drosophila. Dev. Cell 9: 511–522. https://doi.org/10.1016/j.devcel.2005.09.002

Bienkowski, R. S., A. Banerjee, J. C. Rounds, J. Rha, O. F. Omotade et al., 2017 The Conserved, Disease-Associated RNA Binding Protein dNab2 Interacts with the Fragile X Protein Ortholog in Drosophila Neurons. Cell Rep. 20: 1372–1384. https://doi.org/10.1016/j.celrep.2017.07.038

Boutros, M., N. Paricio, D. I. Strutt, and M. Mlodzik, 1998 Dishevelled activates JNK and discriminates between JNK pathways in planar polarity and wingless signaling. Cell 94: 109–118. https://doi.org/10.1016/S0092-8674(00)81226-X

Castello, A., B. Fischer, M. W. Hentze, and T. Preiss, 2013 RNA-binding proteins in Mendelian disease. Trends Genet. 29: 318–327. https://doi.org/10.1016/j.tig.2013.01.004

Cohen, E. D., M. C. Mariol, R. M. Wallace, J. Weyers, Y. G. Kamberov et al., 2002 DWnt4 regulates cell movement and focal adhesion kinase during Drosophila ovarian morphogenesis. Dev. Cell 2: 437–448. https://doi.org/10.1016/S1534-5807(02)00142-9

Collins, S. C., A. Mikhaleva, K. Vrcelj, V. E. Vancollie, C. Wagner et al., 2019 Large-scale neuroanatomical study uncovers 198 gene associations in mouse brain morphogenesis. Nat. Commun. 10: 3465. https://doi.org/10.1038/s41467-019-11431-2

Fasken, M. B., and A. H. Corbett, 2016 Links between mRNA splicing, mRNA quality control, and intellectual disability. RNA Dis. 3: e1448.

Gombos, R., E. Migh, O. Antal, A. Mukherjee, A. Jenny et al., 2015 The Formin DAAM Functions as Molecular Effector of the Planar Cell Polarity Pathway during Axonal Development in Drosophila. J. Neurosci. 35: 10154–10167. https://doi.org/10.1523/JNEUROSCI.3708-14.2015

Green, C., E. Levashina, C. McKimmie, T. Dafforn, J. M. Reichhart et al., 2000 The necrotic gene in Drosophila corresponds to one of a cluster of three serpin transcripts mapping at 43A1.2. Genetics 156: 1117–1127.

Gubb, D., C. Green, D. Huen, D. Coulson, G. Johnson et al., 1999 The balance between isoforms of the prickle LIM domain protein is critical for planar polarity in Drosophila imaginal discs. Genes Dev. 13: 2315–2327. https://doi.org/10.1101/gad.13.17.2315

Guthrie, C. R., L. Greenup, J. B. Leverenz, and B. C. Kraemer, 2011 MSUT2 is a determinant of susceptibility to tau neurotoxicity. Hum. Mol. Genet. 20: 1989–1999. https://doi.org/10.1093/hmg/ddr079

Haelterman, N. A., L. Jiang, Y. Li, V. Bayat, H. Sandoval et al., 2014 Large-scale identification of chemically induced mutations in Drosophila melanogaster. Genome Res. 24: 1707–1718. https://doi.org/10.1101/gr.174615.114

Hollis, 2nd, E. R., and Y. Zou, 2012 Expression of the Wnt signaling system in central nervous system axon guidance and regeneration. Front. Mol. Neurosci. 5: 5. https://doi.org/10.3389/fnmol.2012.00005

Inaki, M., S. Yoshikawa, J. B. Thomas, H. Aburatani, and A. Nose, 2007 Wnt4 is a local repulsive cue that determines synaptic target specificity. Curr. Biol. 17: 1574–1579. https://doi.org/10.1016/j.cub.2007.08.013

Kelly, S. M., R. Bienkowski, A. Banerjee, D. J. Melicharek, Z. A. Brewer et al., 2016 The Drosophila ortholog of the Zc3h14 RNA binding protein acts within neurons to pattern axon projection in the developing brain. Dev. Neurobiol. 76: 93–106. https://doi.org/10.1002/dneu.22301

Kelly, S. M., S. W. Leung, C. Pak, A. Banerjee, K. H. Moberg et al., 2014 A conserved role for the zinc finger polyadenosine RNA binding protein, ZC3H14, in control of poly(A) tail length. RNA 20: 681–688. https://doi.org/10.1261/rna.043984.113

Leung, S. W., L. H. Apponi, O. E. Cornejo, C. M. Kitchen, S. R. Valentini et al., 2009 Splice variants of the human ZC3H14 gene generate multiple isoforms of a zinc finger polyadenosine RNA binding protein. Gene 439: 71–78. https://doi.org/10.1016/j.gene.2009.02.022

Liu, M., Y. Li, A. Liu, R. Li, Y. Su et al., 2016 The exon junction complex regulates the splicing of cell polarity gene dlg1 to control Wingless signaling in development. eLife 5: e17200. https://doi.org/10.7554/eLife.17200

Lu, B., T. Usui, T. Uemura, L. Jan, and Y. N. Jan, 1999 Flamingo controls the planar polarity of sensory bristles and asymmetric division of sensory organ precursors in Drosophila. Curr. Biol. 9: 1247–1250. https://doi.org/10.1016/S0960-9822(99)80505-3

Luo, L., T. Tully, and K. White, 1992 Human amyloid precursor protein ameliorates behavioral deficit of flies deleted for Appl gene. Neuron 9: 595–605. https://doi.org/10.1016/0896-6273(92)90024-8

Martin-Blanco, E., A. Gampel, J. Ring, K. Virdee, N. Kirov et al., 1998 puckered encodes a phosphatase that mediates a feedback loop regulating JNK activity during dorsal closure in Drosophila. Genes Dev. 12: 557–570. https://doi.org/10.1101/gad.12.4.557

Mora, N., I. Almudi, B. Alsina, M. Corominas, and F. Serras, 2013 β amyloid protein precursor-like (Appl) is a Ras1/MAPK-regulated gene required for axonal targeting in Drosophila photoreceptor neurons. J. Cell Sci. 126: 53–59. https://doi.org/10.1242/jcs.114785

Morgan, T. H., Bridges, C.B. and Sturtevant, A.H., 1925 The genetics of Drosophila melanogaster.

Morris, K. J., and A. H. Corbett, 2018 The polyadenosine RNA-binding protein ZC3H14 interacts with the THO complex and coordinately regulates the processing of neuronal transcripts. Nucleic Acids Res. 46: 6561–6575. https://doi.org/10.1093/nar/gky446

Morrison, H. A., H. Dionne, T. E. Rusten, A. Brech, W. W. Fisher et al., 2008 Regulation of early endosomal entry by the Drosophila tumor suppressors Rabenosyn and Vps45. Mol. Biol. Cell 19: 4167–4176. https://doi.org/10.1091/mbc.e08-07-0716

Mottola, G., A. K. Classen, M. Gonzalez-Gaitan, S. Eaton, and M. Zerial, 2010 A novel function for the Rab5 effector Rabenosyn-5 in planar cell polarity. Development 137: 2353–2364. https://doi.org/10.1242/dev.048413

Nagarkar-Jaiswal, S., P. T. Lee, M. E. Campbell, K. Chen, S. Anguiano-Zarate et al., 2015 A library of MiMICs allows tagging of genes and reversible, spatial and temporal knockdown of proteins in Drosophila. eLife 4: e05338. https://doi.org/10.7554/eLife.05338

Ng, J., 2012 Wnt/PCP proteins regulate stereotyped axon branch extension in Drosophila. Development 139: 165–177. https://doi.org/10.1242/dev.068668

Pak, C., M. Garshasbi, K. Kahrizi, C. Gross, L. H. Apponi et al., 2011 Mutation of the conserved polyadenosine RNA binding protein, ZC3H14/dNab2, impairs neural function in Drosophila and humans. Proc. Natl. Acad. Sci. USA 108: 12390–12395. https://doi.org/10.1073/pnas.1107103108

Park, W. J., J. Liu, and P. N. Adler, 1994 The frizzled gene of Drosophila encodes a membrane protein with an odd number of transmembrane domains. Mech. Dev. 45: 127–137. https://doi.org/10.1016/0925-4773(94)90026-4

Penton, A., A. Wodarz, and R. Nusse, 2002 A mutational analysis of dishevelled in Drosophila defines novel domains in the dishevelled protein as well as novel suppressing alleles of axin. Genetics 161: 747–762.

G3·Genes|Genomes|Genetics

Perrimon, N., and A. P. Mahowald, 1987   Multiple functions of segment polarity genes in Drosophila. Dev. Biol. 119: 587–600. https://doi.org/10.1016/0012-1606(87)90061-3

Povelones, M., R. Howes, M. Fish, and R. Nusse, 2005   Genetic evidence that Drosophila frizzled controls planar cell polarity and Armadillo signaling by a common mechanism. Genetics 171: 1643–1654. https://doi.org/10.1534/genetics.105.045245

Rawls, A. S., and T. Wolff, 2003   Strabismus requires Flamingo and Prickle function to regulate tissue polarity in the Drosophila eye. Development 130: 1877–1887. https://doi.org/10.1242/dev.00411

Rha, J., S. K. Jones, J. Fidler, A. Banerjee, S. W. Leung *et al.*, 2017   The RNA-binding Protein, ZC3H14, is Required for Proper Poly(A) Tail Length Control, Expression of Synaptic Proteins, and Brain Function in Mice. Hum Mol Genet. 26: 3663–3681. https://doi.org/10.1093/hmg/ddx248

Sato, M., D. Umetsu, S. Murakami, T. Yasugi, and T. Tabata, 2006   DWnt4 regulates the dorsoventral specificity of retinal projections in the Drosophila melanogaster visual system. Nat. Neurosci. 9: 67–75. https://doi.org/10.1038/nn1604

Soldano, A., Z. Okray, P. Janovska, K. Tmejova, E. Reynaud *et al.*, 2013   The Drosophila homologue of the amyloid precursor protein is a conserved modulator of Wnt PCP signaling. PLoS Biol. 11: e1001562. https://doi.org/10.1371/journal.pbio.1001562

Soucek, S., Y. Zeng, D. L. Bellur, M. Bergkessel, K. J. Morris *et al.*, 2016   The Evolutionarily-conserved Polyadenosine RNA Binding Protein, Nab2, Cooperates with Splicing Machinery to Regulate the Fate of pre-mRNA. Mol Cell Biol. 36: 2697–2714. https://doi.org/10.1128/MCB.00402-16

Srahna, M., M. Leyssen, C. M. Choi, L. G. Fradkin, J. N. Noordermeer *et al.*, 2006   A signaling network for patterning of neuronal connectivity in the Drosophila brain. PLoS Biol. 4: e348. https://doi.org/10.1371/journal.pbio.0040348

Torroja, L., M. Packard, M. Gorczyca, K. White, and V. Budnik, 1999   The Drosophila beta-amyloid precursor protein homolog promotes synapse differentiation at the neuromuscular junction. J. Neurosci. 19: 7793–7803. https://doi.org/10.1523/JNEUROSCI.19-18-07793.1999

van den Bogaart, G., A. C. Meinema, V. Krasnikov, L. M. Veenhoff, and B. Poolman, 2009   Nuclear transport factor directs localization of protein synthesis during mitosis. Nat. Cell Biol. 11: 350–356. https://doi.org/10.1038/ncb1844

Vandewalle, J., M. Langen, M. Zschatzsch, B. Nijhof, J. M. Kramer *et al.*, 2013   Ubiquitin ligase HUWE1 regulates axon branching through the Wnt/beta-catenin pathway in a Drosophila model for intellectual disability. PLoS One 8: e81791. https://doi.org/10.1371/journal.pone.0081791

Wolff, T., and G. M. Rubin, 1998   Strabismus, a novel gene that regulates tissue polarity and cell fate decisions in Drosophila. Development 125: 1149–1159.

Xu, W., 2011   PSD-95-like membrane associated guanylate kinases (PSD-MAGUKs) and synaptic plasticity. Curr. Opin. Neurobiol. 21: 306–312. https://doi.org/10.1016/j.conb.2011.03.001

Yanagawa, S., F. van Leeuwen, A. Wodarz, J. Klingensmith, and R. Nusse, 1995   The dishevelled protein is modified by wingless signaling in Drosophila. Genes Dev. 9: 1087–1097. https://doi.org/10.1101/gad.9.9.1087

Yang, Y., and M. Mlodzik, 2015   Wnt-Frizzled/planar cell polarity signaling: cellular orientation by facing the wind (Wnt). Annu. Rev. Cell Dev. Biol. 31: 623–646. https://doi.org/10.1146/annurev-cellbio-100814-125315

Yuan, L., S. Hu, Z. Okray, X. Ren, N. De Geest *et al.*, 2016   The Drosophila neurogenin Tap functionally interacts with the Wnt-PCP pathway to regulate neuronal extension and guidance. Development 143: 2760–2766. https://doi.org/10.1242/dev.134155

Communicating editor: H. Salz